

ARTIFICIAL NEURAL NETWORK CONTROL OF VECTOR CONTROLLED INDUCTION MOTOR

YASSER G. DESSOUKY¹, MONA F. MOUSSA² and EZZ EL_DIEN ZAKZOUK³

ABSTRACT

Many researches have been carried out to induction motors for starting, braking, speed reversal and speed control, because they are relatively cheap, reliable and rugged machines due to absence of slip rings or commutators. Induction motors exhibit highly coupled, nonlinear time varying system which is difficult to control since some state variables are difficult to be measured. However, recent advancements in semiconductor power electronics and microcontrollers have made it possible to use induction motors in many variable speed drive applications, as they are capable of similar performance as DC motor. This paper presents a study for indirect vector control of induction motor as it can be operated over a wide speed range, including low speed, with rapid, accurate torque control and good momentary overload capabilities. Also, the use of artificial neural network, ANN is proposed to emulate the function of Indirect-Field-Oriented-Control (IFOC), to perform the critical function of synchronous speed estimation internally, transformation from three-phase ABC currents to two-phase d-q synchronous frame currents and transformation from two-phase d-q synchronous frame voltages to three-phase ABC voltages during both constant torque and constant power regions, also for motor reversing and braking modes.

KEYWORDS: Induction motor, vector control, artificial neural network

¹ Assistant Professor

² Engineer

³ Professor of the Arab Academy for Science and Technology, Department of Electrical and Control Engineering, Miami, Alexandria, P.O. Box: 1024, Egypt.

1. INTRODUCTION

In order to generate the highest possible torque per ampere of stator current and hence the best possible utilization of the available current capability of the induction, motor flux level must be kept constant and close to its nominal value as the motor operating conditions vary. Therefore, the two controllable parameters (stator supply voltage and frequency) have to be adjusted for each operating condition. Several techniques of controlling speed of the induction motor are now available such as, V/f control [1], stator current and slip frequency scalar control [2], direct [3] and indirect vector control [4] and direct torque control [5]. Vector control provides highest possible control performance for an induction machine, as the stator current or voltage space phasors are controlled in magnitude and position, by using a twin-axis synchronously rotating reference frame aligned with the flux vector. The stator current can be split up into a flux producing component and a torque-producing component, both of which are DC values at steady state. This allows decoupled control of flux and torque, similar to that of a separately excited DC machine. The flux producing current component (d -axis) provides a slow response mechanism to change the flux in the machine, while the torque producing current component (q -axis) allows fast controlled changes of torque [6]. With this arrangement, the control dynamics of the highly coupled nonlinear structure of the induction machine becomes linearized, as it loses all the sinusoidal terms and becomes decoupled since the active and reactive components of current are perpendicular and have no mutual effects. Several methods have been proposed to implement field-oriented control [4-7] as it is possible to operate over a wide speed range, from standstill to well over the rated base speed, in either direction, and still maintain full control of the torque produced. In addition, dynamic braking, or regeneration is easily implemented which means that; it is easy to regenerate the mechanical power of the rotor shaft back into the supply. Vector control is achieved by estimating, measuring or calculating the magnitude and position of the flux in the machine. Then, the stator current phasor can be aligned to maintain the field at the desired level, and to produce torque as desired. A reference synchronous frame conversion is used to split the stator current into the flux

producing component and the torque-producing component. In the indirect method of vector control, the slip angle, θ_{sl} which is defined as the difference between the rotor θ_r and the synchronous angle, θ_e is calculated using the measured stator current and rotor speed, giving the position of the rotor flux-linkage when added to the rotor angle. This method heavily depends on the rotor time constant. It avoids the requirement of flux acquisition by using known motor parameters to compute the appropriate motor slip frequency to obtain the desired flux position. This scheme is more popular because it is simpler to implement than the direct method of field oriented control. Moreover, decoupled flux and torque control has the ability to reduce the flux at low loads. This increases both the motor and inverter efficiencies compared to a machine operating directly from the mains, while still maintaining the required torque. The application of ANN to various aspects of induction motor control has been investigated, such as adaptive control [8], sensorless speed control [9], inverter current regulation [10], as well as for motor parameter identification purposes [11], and flux estimation purposes. ANN technique is based on learning process and it has the advantage of extremely fast parallel computation and fault tolerance characteristics due to distributed network intelligence. Furthermore, it is capable of handling time varying nonlinearities due to its own nonlinear nature. Therefore, the use of ANN to emulate the function of indirect-field-oriented-control (IFOC) has been proposed, since ANNs can create their own organization of the information they receive during learning time, and have immunity from input harmonic ripple and ability to be used as lookup table without delay. The feed forward multilayer network is used, where no information is fed back during learning process. The back propagation algorithm is used for adjusting the weights, and biases during training [12]. ANN performs critical function of synchronous speed estimation, voltage transformation from synchronous to stationary frame and current transformation from stationary to synchronous frame.

2. SYSTEM DYNAMICS AND SIMULATIONS

The differential equations of the induction motor, in the synchronously rotating reference frame, are derived as follows [6]:

$$V_{dr} = R_r i_{dr}^e + \frac{d\psi_{dr}^e}{dt} + (\omega_e - \omega_r)\psi_{qr}^e = 0 \quad (1)$$

$$V_{qr} = R_r i_{qr}^e + \frac{d\psi_{qr}^e}{dt} - (\omega_e - \omega_r)\psi_{dr}^e = 0 \quad (2)$$

The flux linkage expressions in terms of the stator and rotor currents will be:

$$\frac{d\psi_{qr}^e}{dt} = \frac{L_m}{T_r} i_{qs}^e - \frac{1}{T_r} \psi_{qr}^e - (\omega_e - \omega_r)\psi_{dr}^e \quad (3)$$

$$\frac{d\psi_{dr}^e}{dt} = \frac{L_m}{T_r} i_{ds}^e - \frac{1}{T_r} \psi_{dr}^e + (\omega_e - \omega_r)\psi_{qr}^e \quad (4)$$

Where T_r is the rotor time constant (L_r/R_r). For vector control, the d- axis of the synchronous frame is aligned with the rotor flux and therefore:

$$\psi_{qr}^e = \frac{d\psi_{qr}^e}{dt} = 0 \quad (5)$$

Also, this implies the following:

$$\psi_{dr}^e = \psi_r = \text{constant} \quad (6)$$

$$\frac{d\psi_{dr}^e}{dt} = \frac{d\psi_r}{dt} = 0 \quad (7)$$

Substituting Eq. (5) into Eq. (3) and Eq. (2) and rearranging to get:

$$\frac{d\psi_r}{dt} = \frac{L_m}{T_r} i_{ds}^e - \frac{1}{T_r} \psi_r \quad (8)$$

$$\omega_{sl} = \omega_e - \omega_r = \left(\frac{L_m}{T_r}\right) \frac{i_{qs}^e}{\psi_r} \quad (9)$$

The calculations required to implement indirect vector control are given by both Eq. (8) which represents the rotor flux magnitude and Eq. (9) which represents the slip speed which when integrated, with zero initial condition, gives the slip position [i.e.: the rotor flux position relative to the rotor position]. The absolute flux position is found by adding the slip position to the rotor position, which is used in the conversion from the synchronous to the stationary frame. Applying Laplace transform to Eq. (8), the transfer function $G(s)$, which has an input of i_{ds}^e , and output of ψ_r , can be expressed as follows:

$$G(s) = \frac{\psi_r(s)}{i_{ds}^e(s)} = \frac{L_m}{T_r \left(s + \frac{1}{T_r} \right)} \quad (10)$$

Figure 1 shows a schematic diagram for the indirect voltage vector implementation on the induction machine. After being measured, the three phase stator currents are converted into stationary frame using Eq. (11) and then to synchronously rotating frame stator currents as in Eq. (12) [6]. The two command currents (i_{ds}^{e*} and i_{qs}^{e*}) are compared with the actual currents (i_{ds}^e and i_{qs}^e) and the errors are implemented to the P-type current controllers whose outputs are the synchronously rotating frame d^e - q^e stator voltages (v_{ds}^e and v_{qs}^e) which in turn are converted into stationary frame stator voltage as in Eq. (13) and then into three phase reference voltages using Eq. (14). The three-phase inverter realizes the three phase PWM voltages on the motor phases.

$$\begin{aligned} i_{ds}^s &= i_a \\ i_{qs}^s &= -\frac{1}{2}i_a + \frac{\sqrt{3}}{2}i_b - \frac{\sqrt{3}}{2}i_c \end{aligned} \quad (11)$$

$$\begin{aligned} i_{ds}^e &= i_{ds}^s \cos(\theta_e) + i_{qs}^s \sin(\theta_e) \\ i_{qs}^e &= -i_{ds}^s \sin(\theta_e) + i_{qs}^s \cos(\theta_e) \end{aligned} \quad (12)$$

$$\begin{aligned} v_{ds}^s &= v_{ds}^e \cos(\theta_e) - v_{qs}^e \sin(\theta_e) \\ v_{qs}^s &= v_{ds}^e \sin(\theta_e) + v_{qs}^e \cos(\theta_e) \end{aligned} \quad (13)$$

$$\begin{aligned} V_a &= v_{ds}^s \\ V_b &= -\frac{1}{2}v_{ds}^s + \frac{\sqrt{3}}{2}v_{qs}^s \\ V_c &= -\frac{1}{2}v_{ds}^s - \frac{\sqrt{3}}{2}v_{qs}^s \end{aligned} \quad (14)$$

3. STRUCTURE OF THE PROPOSED NEURAL NETWORK

The neural network performs the critical functions of synchronous speed estimation, voltage transformation from synchronous to stationary frame, and current transformation from stationary to synchronous frame. The conventional neural network architecture is not well suited for patterns that vary over time. The prototypical use of neural networks is in structural pattern recognition. In such task,

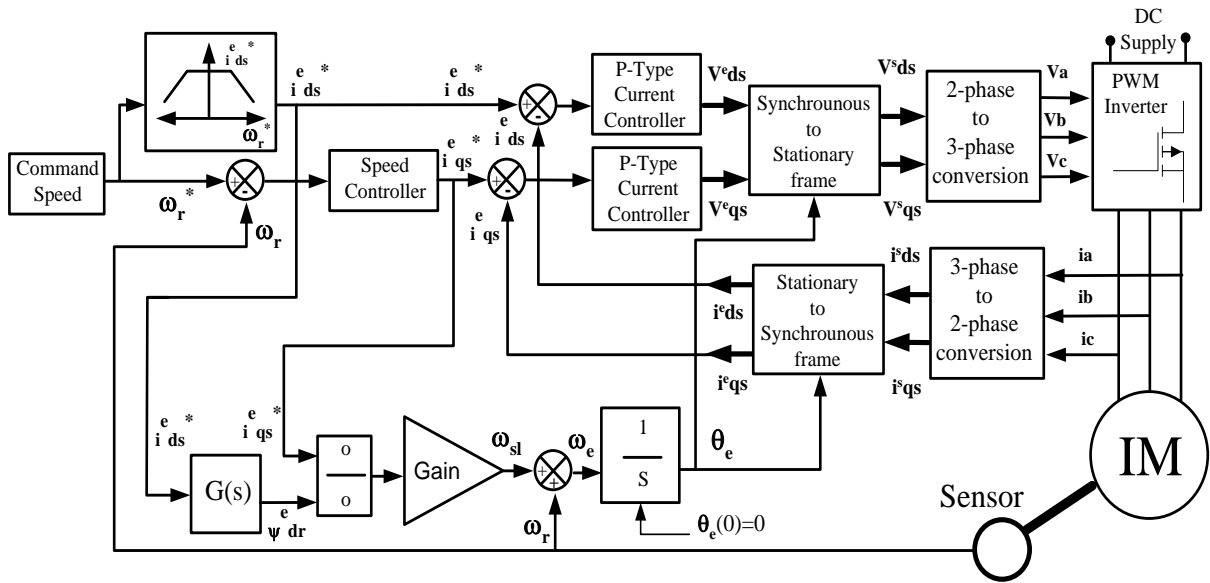


Fig. 1. Block diagram of the indirect field oriented control induction motor.

The network uses a collection of features presented to classify the input feature patterns into classes. In this method, the network is presented with all relevant information simultaneously. In contrast, temporal pattern recognition involves processing of patterns that evolve over time. Samples of speed, voltage and current waveforms, which are time-varying signals, are usually used as inputs to the neural network. Therefore, a network with temporal processing abilities (feed forward ANN with delay operator Z^{-1} which store values from the previous time step, to be used in the current time step) should be considered. A TANSIG nonlinear activation function was chosen for both hidden and output layers of the network, because it helps in producing an arbitrary decision with smooth curves and edges. Also it has the ability to produce positive or negative outputs [12].

3.1 Synchronous speed estimation

The synchronous speed is estimated using a neural network whose three inputs are: the torque producing command current, i_{qs}^* , the flux producing command current, i_{ds}^* and the rotor speed signal, ω_r . The inputs are normalized in order to keep the value of the variables in the network between ± 1 . The output of the neural network is

the synchronous velocity (ω_e). The network is fully connected. In addition, a bias signal is coupled to all the neurons through a weight. The number of samples inputting to the neural network and the number of neurons in the hidden layer were decided by trial and error process that involved training and testing different network configurations. The process was terminated when a suitable network with satisfactory performance was established. The performance of the network was checked in terms of computational requirements, generalization capability, response time and fault tolerance. First, an ANN with three layers is proposed where the input layer has three neurons, the hidden layer has ten neurons, and the output layer has one neuron. The three layers network is trained for several forward and reverse speed step command signal but this ANN structure was not satisfactory. The neural network accuracy can be improved by increasing the number of hidden layers, the number of neurons, or increasing the training time. The selection of hidden layer neurons may require several stages of iteration. If the number is small, the error will not converge to the satisfactory level, while if the number is large, the network tends to memorize rather than learn. Various networks were trained and tested. By a trial and error process, satisfactory results were obtained with nine neurons in the input layer. These inputs are [i_{qs}^e *, i_{ds}^e * and ω_r] making a total of three inputs where each input is represented by three consecutive previous samples. The proposed ANN has two hidden layers. The number of neurons in the first and the second hidden are 12 and 6 neurons, respectively. Finally, it is found that, the simplest four layers design $N_{9,12,6,1}$ shown in fig. 2 gives acceptable results in convenient time.

3.2 Voltage transformation from synchronous to stationary frame

A neural network is used to transform the two dc synchronous frame voltages V_{ds}^e and V_{qs}^e , to the two-phase sinusoidal stationary frame voltages V_{ds}^s and V_{qs}^s which then are converted to the three phase voltages V_{abc} using the relations given in Eq. (13). That means the ANN performs also numerically the function of the integrator shown in fig. (1) with zero initial condition. It should be noted that converting two phase sinusoidal voltages to three phase sinusoidal voltages is performed outside the ANN

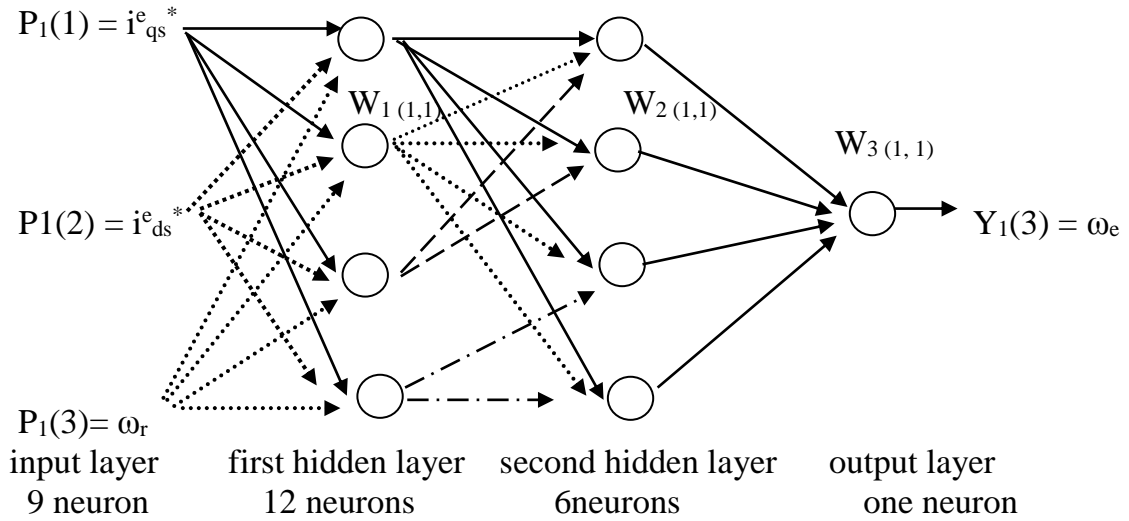


Fig. 2. Architectural graph of the slip estimator neural network $N_{9,12,6,1}$

to simplify its structure. The ANN has three inputs as follows, the d-axis synchronous stator voltage, V_{ds}^e , the q-axis synchronous stator voltage, V_{qs}^e and the synchronous speed, ω_e , and it has two outputs, namely, the d-axis stationary stator voltage, V_{ds}^s and the q-axis stationary stator voltage, V_{qs}^s . By a trial and error process, satisfactory results were obtained with three neurons in the input layer, one hidden layer with nine neurons and two neurons in the output layer (i.e. $N_{3,9,2}$) as shown in fig. 3.

3.3 Current transformation from stationary to synchronous frame

The three phase sinusoidal currents i_{abc} are converted to two phase sinusoidal currents using the relations given in Eq. (11). An ANN network is used to transform the two sinusoidal stationary frame currents to the two dc synchronous frame currents. The ANN has three inputs as follows: the d - axis stationary stator current, i_{ds}^s , the q- axis

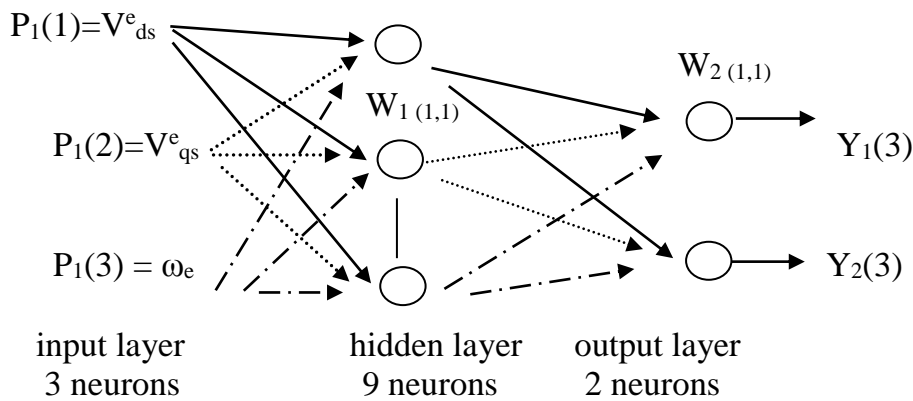


Fig. 3. Architectural graph of the voltage estimator neural network $N_{3,9,2}$.

stationary stator current, i_{qs}^s and the synchronous speed, ω_e and it has two outputs, namely, the d-axis synchronous stator current, i_{ds}^e and the q-axis synchronous stator current, i_{qs}^e . Satisfactory results were obtained with three neurons in the input layer, one hidden layer with six neurons and two neurons in the output layer (i.e. $N_{3,6,2}$) as shown in fig. 4.

4. TRAINING OF ANN

The training data are obtained for several, forward and reverse speed changes and load torque changes, with the aid of SIMULINK software. Since, the number of neurons in an ANN is limited, there is always an error in the output of the network, even when the training data are applied to the ANN. Increasing the number of neurons will decrease this error to a certain limit, adding more neuron to the network after this limit leads to an over fitting problem, in which the response of the network to the training data has smaller error but applying the test data which not used for training) shows large error in the output [12]. The training data are chosen to be roughly in the range of 10% to 120% of the rated speed and for load torque to be in the range of 10% to 120% of rated torque. The network training is highly automated and is usually performed off-line through MATLAB package. To achieve good training and hence good performance of the ANN, during operation, the network should be subjected to the necessary information for speed and torque changes under transient and steady

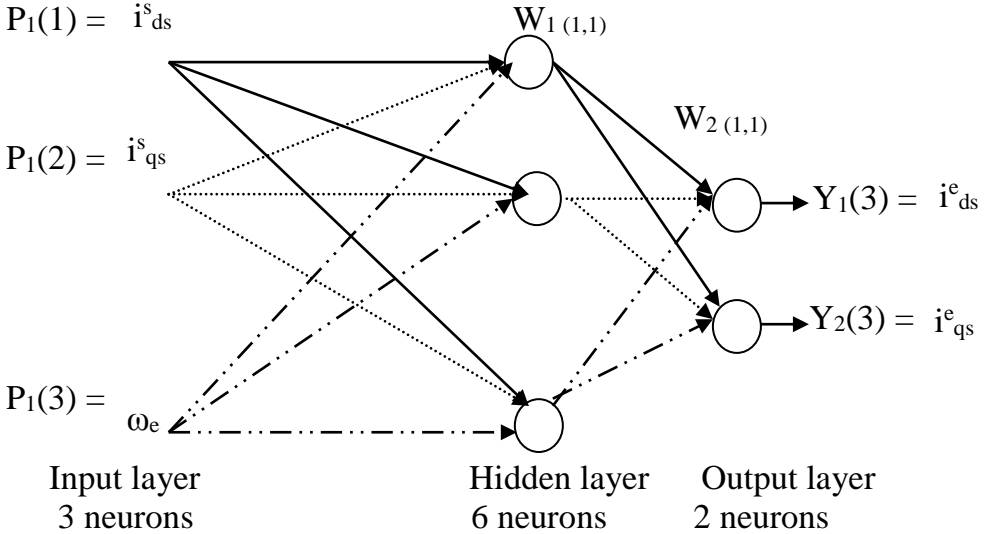
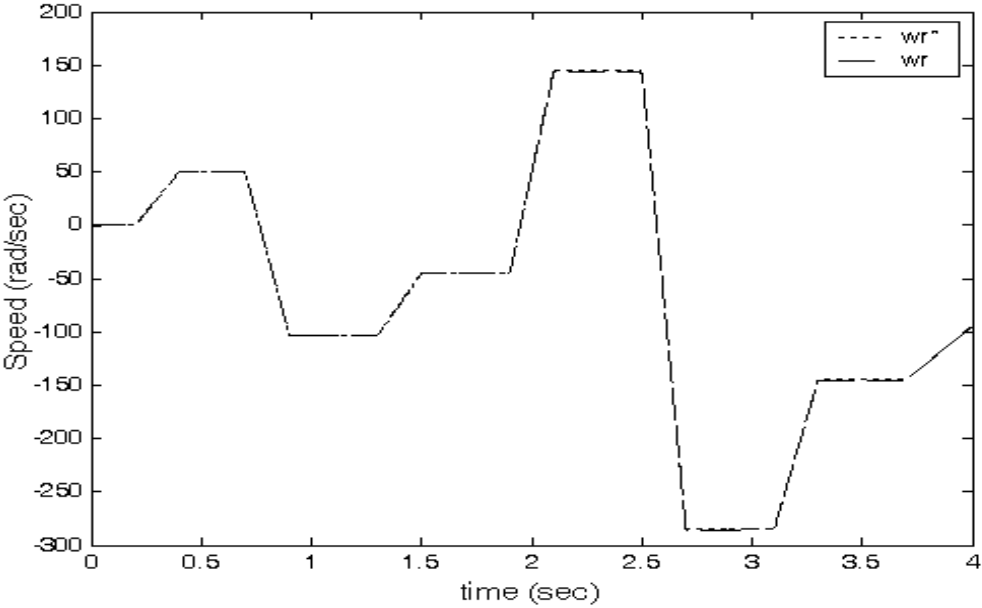
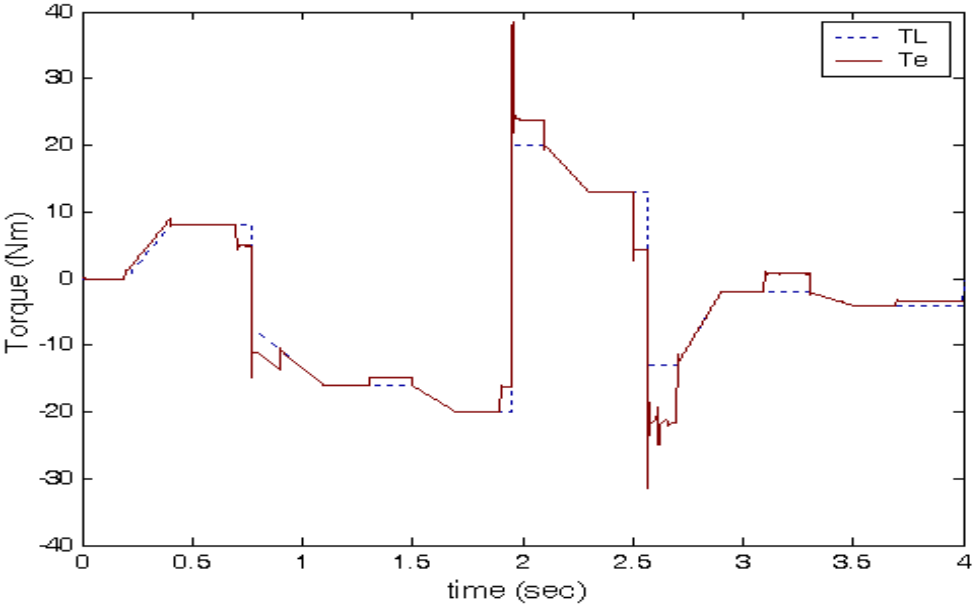


Fig. 4. Architectural graph of the current estimator neural network $N_{3,6,2}$

nominal condition in the wide speed and torque regions. Figure 6 shows the performance of the vector controlled drive system using the proposed ANNs, with a cycled bidirectional speed profile (forward and reverse) and a variable load torque mode, where it is concluded that, the performance of the proposed ANNs is satisfactory, to estimate the slip speed, transform the voltage from synchronous to stationary frame, and the current from stationary to synchronous frame.



(a)

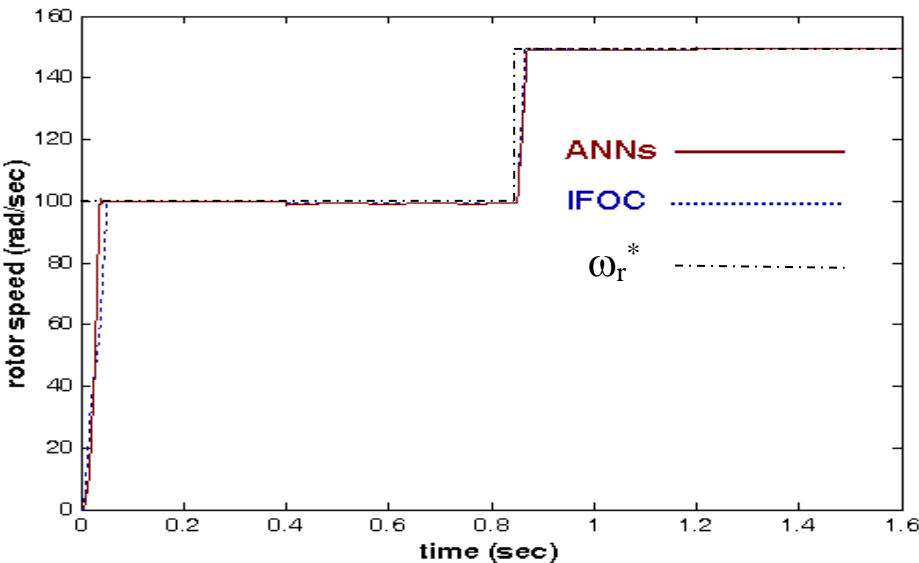


(b)

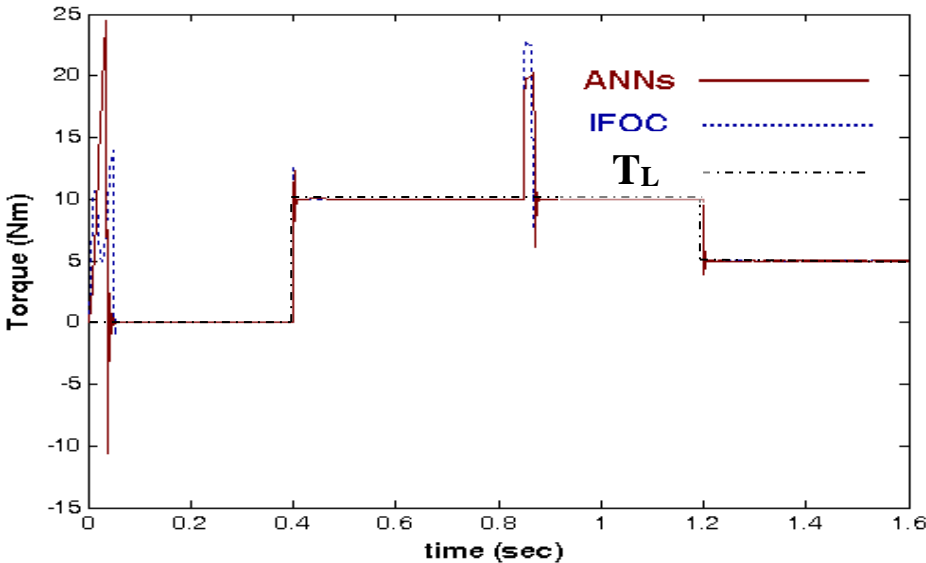
Fig. 6. Relation of time and (a) torque, (b) motor speed.

6. COMPARISON BETWEEN VECTOR CONTROLLED DRIVE AND PROPOSED ANN DRIVES

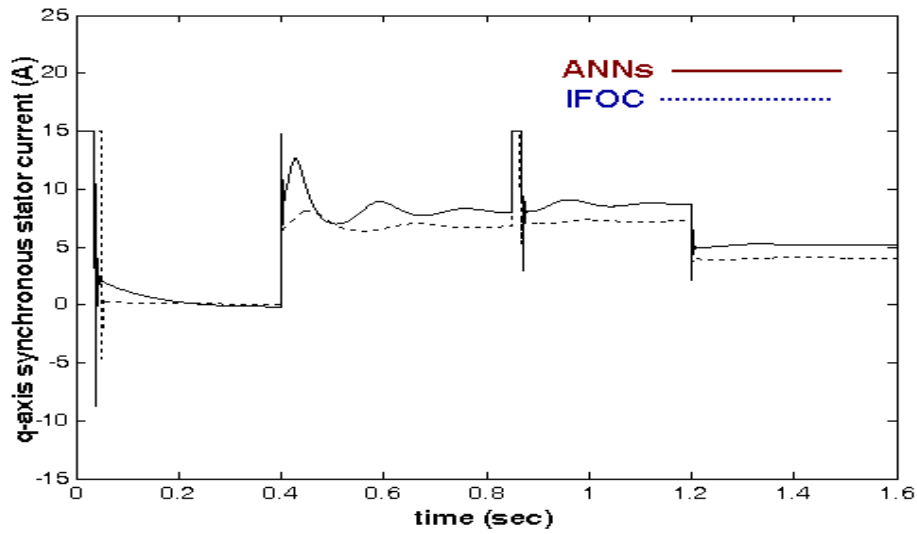
From the above results, the performance of the vector controlled drive system and the proposed neural networks can be compared in different conditions of speed and torque commands as shown in fig. 7. From the depicted figures, it is seen that the proposed neural networks are able to emulate the function of the vector controlled drive system, and give almost the same performance of the conventional IFOC drive system, in terms of torque and speed control. As for fig. (7), before 0.4 sec., both the



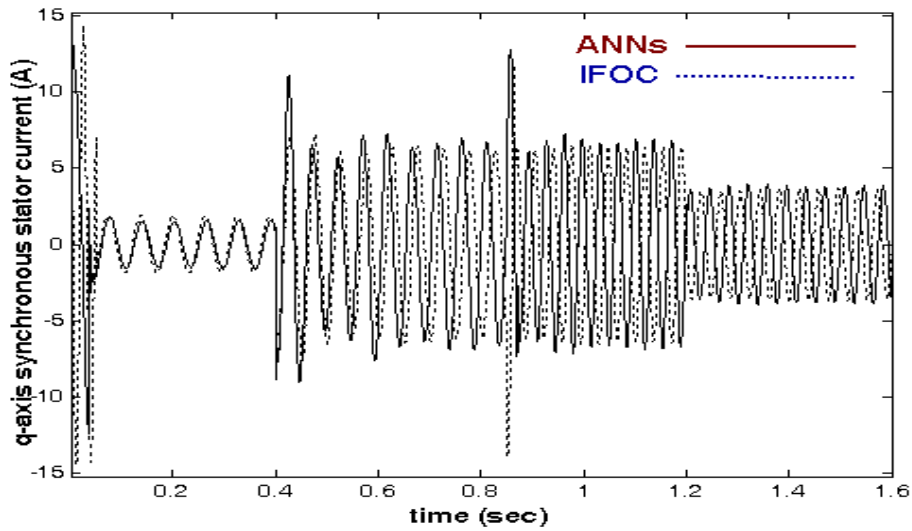
(a)



(b)



(c)



(d)

Fig. 7. Relation of time and (a) ω_r , (b) T_e , (c) i_{qs}^e , (d) i_{qs}^s for both IFOC & ANNs.

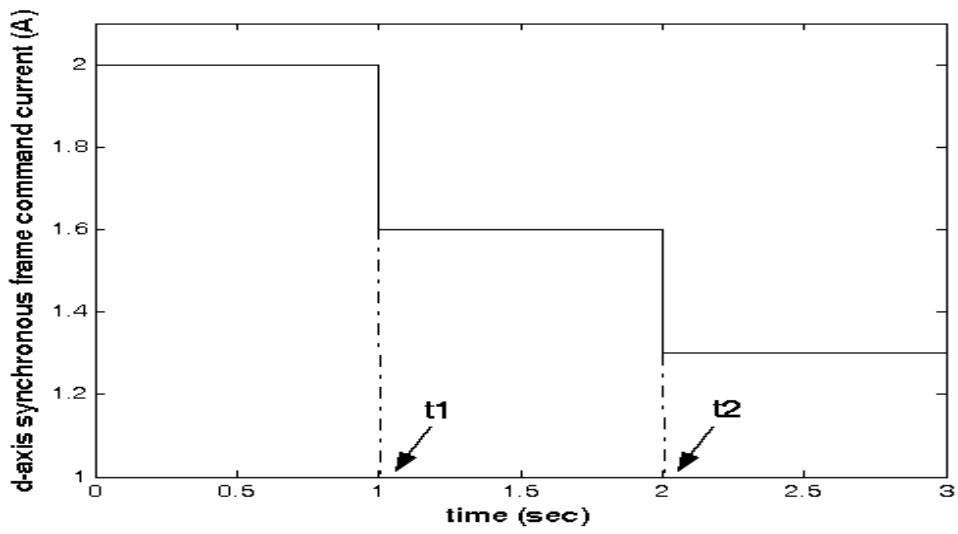
frequency ω_e and the magnitude of the current i_{qs}^s are low corresponding to a command speed of 64% base speed and no load torque respectively, fig (7-d). When the load torque is then applied at 0.4 sec., the magnitude of i_{qs}^s is increased and also the slip speed, and thus frequency ω_e , is increased. When the command speed is increased to base speed at 0.85 sec., the magnitude of i_{qs}^s is not changed as the load torque doesn't but the slip speed, and thus frequency ω_e , is increased. At 1.2 sec., when the load torque is reduced, the magnitude of i_{qs}^s is decreased and the frequency ω_e , is decreased.

7. FIELD WEAKENING MODE

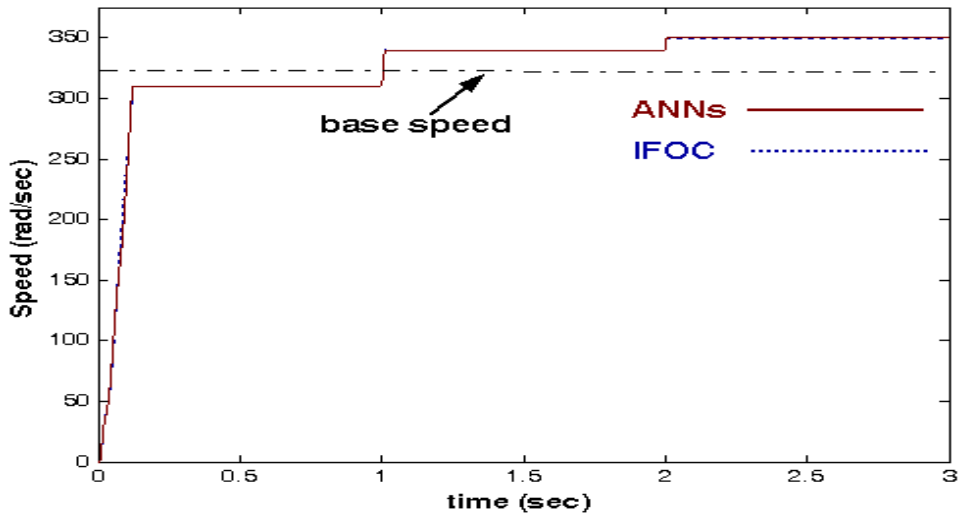
One advantage of using vector control of an induction machine is the capability of operation at speeds above the base speed in the field-weakening region, by driving the machine at its maximum rated voltage, but with a frequency above the rated supply frequency. In vector control, this is achieved by controlling the frequency supplied to the machine; such that the speed is increased by reducing the flux command reference. This results in a weaker field in the machine reducing the back Emf terms analogous to a separately excited DC machine. Below the base speed, the machine operates at constant flux but above the base speed, the flux is weakened inversely proportional to the speed during which, the power available is constant. The disadvantage with field weakening is that the maximum level of torque available is reduced due to the lower rotor flux. With reference to fig. 1, the command current i_{ds}^* is adjusted such that, when the command speed ω_r^* is below the base speed during constant torque region, the command stator current i_{ds}^* is kept constant, whereas, when ω_r^* is above the base speed, the current i_{ds}^* is automatically decreased such that the power is kept constant without exceeding the rated voltage. The proposed ANN has been trained to learn the field weakening operation, above the base speed. Figure 8 shows the comparison between the performances of the machine using vector controlled drive and the proposed ANN in field weakening region. At the time t_1 the command speed ω_r^* is increased from 93% to 105% of base speed and the command d -axis stator current i_{ds}^* is reduced from 100% to 60% of rated value. Again, at time t_2 the command speed is increased from 105% to 110% of base speed and the command d -axis stator current i_{ds}^* is reduced from 60% to 30% of rated value. It is seen that the proposed neural networks are able to operate the induction machine at speeds above the base speed and achieve the same performance of conventional IFOC drive in field weakening region.

8. BRAKING MODE AND REVERSING SPEED

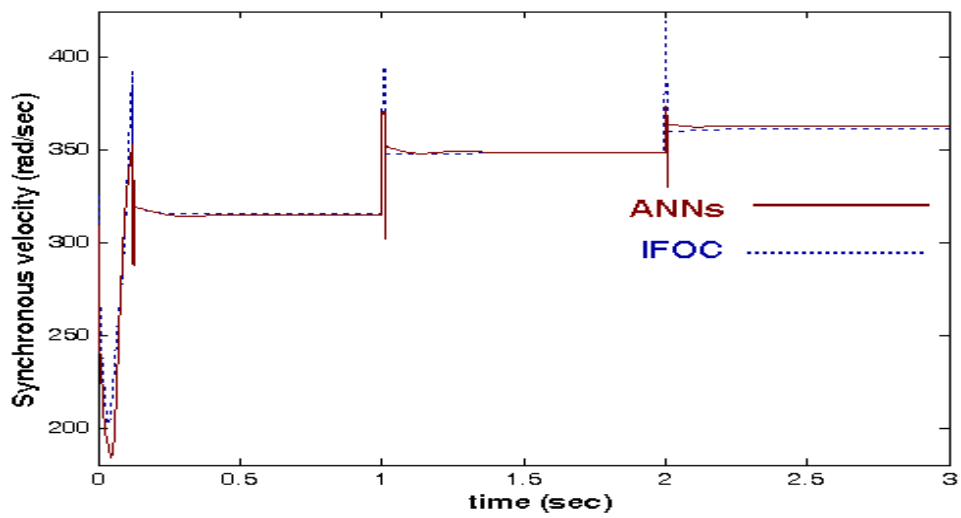
The artificial neural networks ANNs can be also implemented in the braking mode and reversing speed operation. Braking mode can be simulated by reversing the polarity of the command load torque, which leads to reverse the polarity of the q -axis



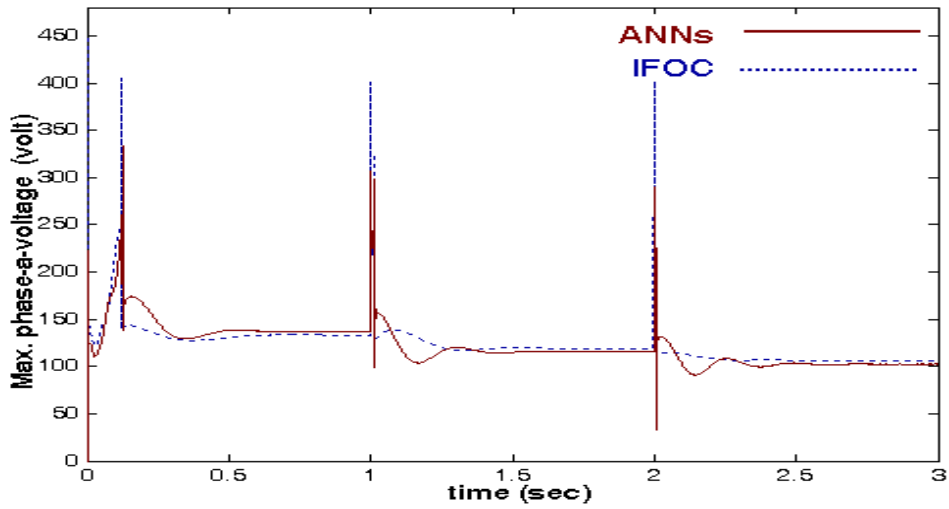
(a)



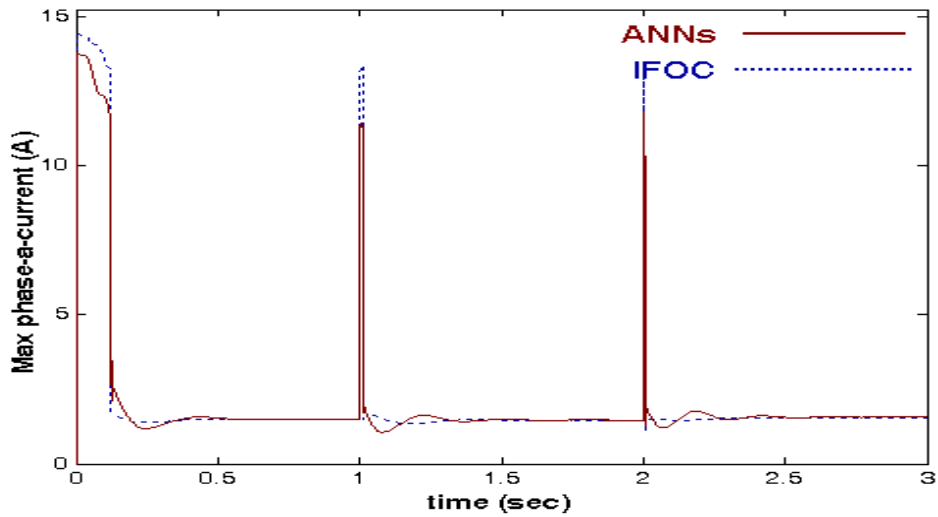
(b)



(c)



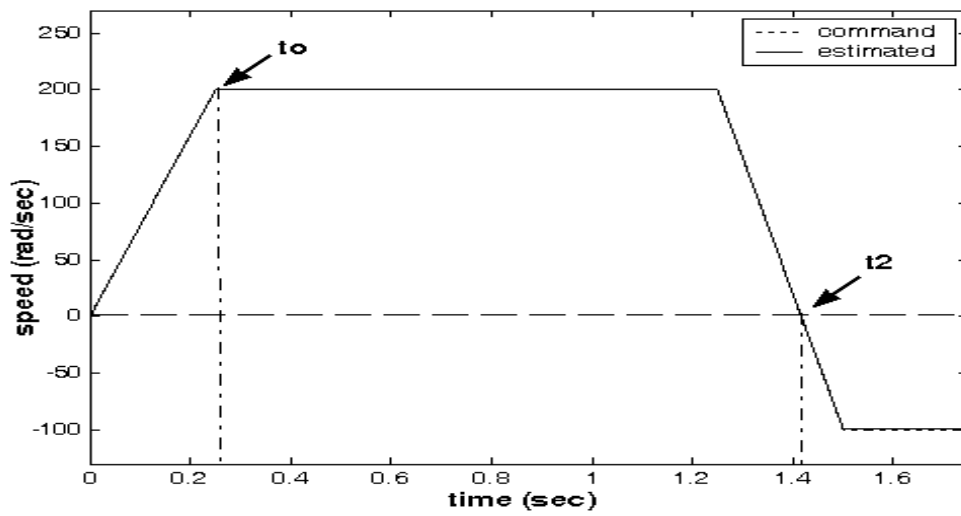
(d)



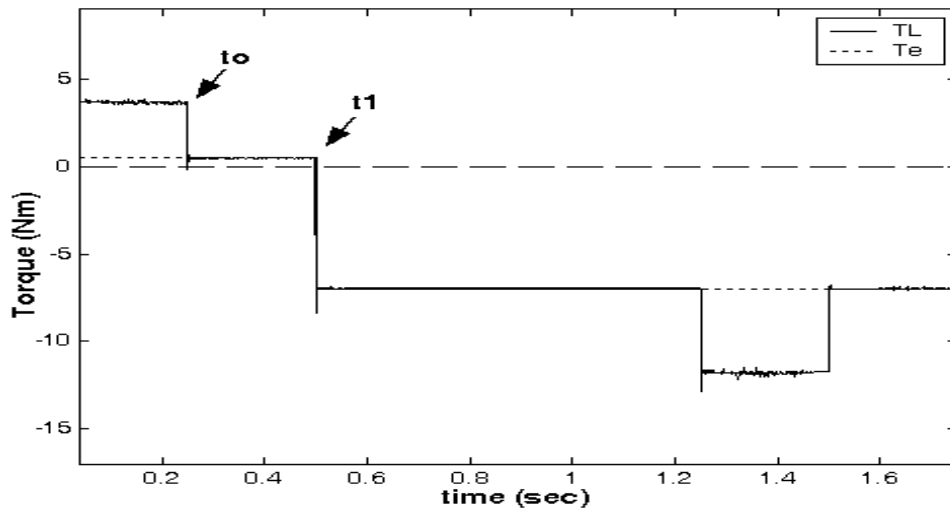
(e)

Fig. 8. Relation of time and (a) i_{ds}^* , (b) ω_r , (c) ω_s , (d) V_{a-max} , (e) i_{a-max} .

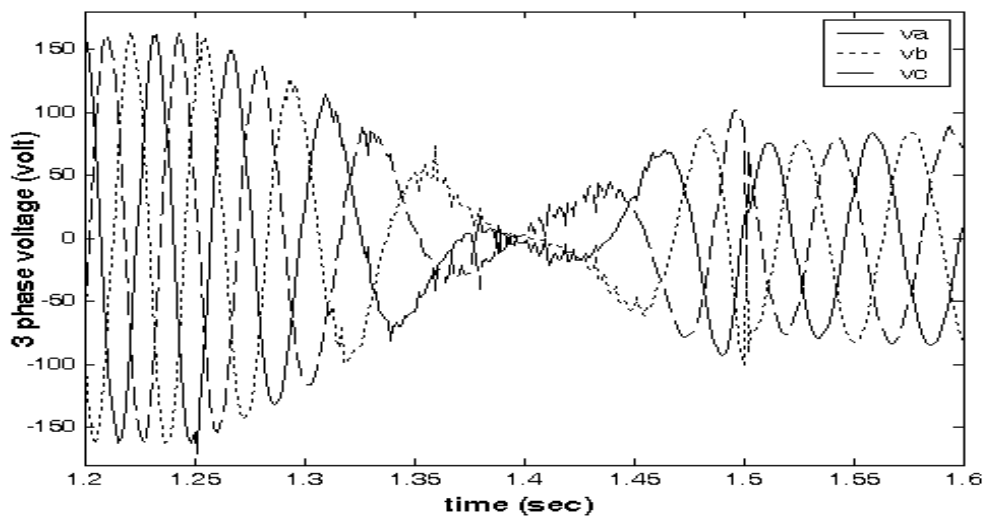
synchronous frame command stator current i_{qs}^* . Figure 9-a shows that the starting at no load is at time t_0 and the command speed signal is reversed at time t_2 . Figure 9-b shows that the command torque is reversed at time t_1 . The motor output speed, ω_r and the electromagnetic output torque T_e track the command signals. Figure 9-c shows that the phase sequence of the three phase voltages is reversed, due to the reverse polarity of the command speed. It may be concluded, from the fig. 9, that the neural network performing the function of the vector controlled drive system, has satisfactory performances in terms of torque and speed control in both directions; forward and



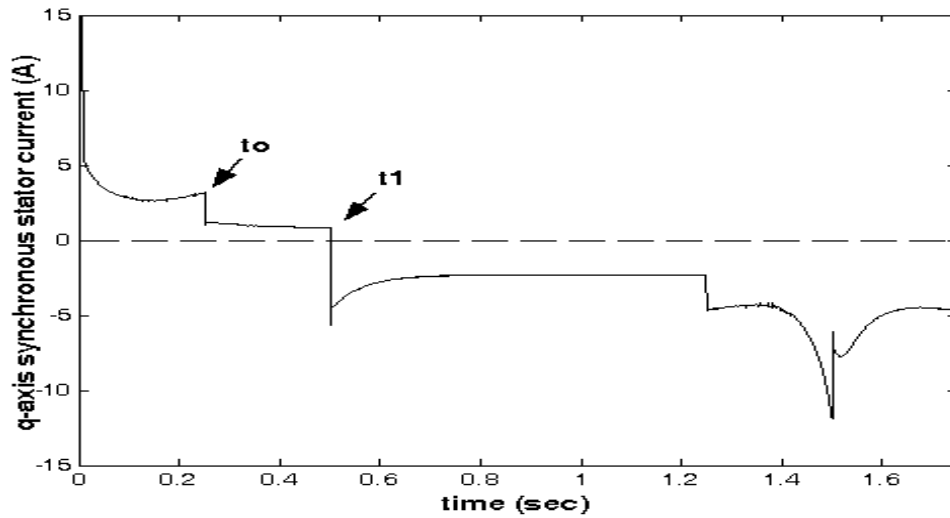
(a)



(b)



(c)



(d)

Fig. 9. Relation of time and (a) output speed, (b) torque, (c) three phase voltages, (d) synchronous stator current.

reverse. Moreover, they can be used in the regenerative braking mode of operation, (i.e. in four quadrant operations).

9. CONCLUSION

Indirect vector controlled of 3-phase induction motor has been studied emphasizing on estimating the slip speed for the indirect field oriented control (IFOC) using the artificial neural network (ANN) as a non-linear regularization technique. One of the most important advantages of the vector control is its ability to change the magnitude, the frequency, and the phase angle of the phase supply voltages. Thus, by applying IFOC to the induction machine, it will behave exactly like a separately excited DC machine, due to the independent control of flux and torque. The performance of the ANN was found to match well at wide speed and torque ranges, in both directions; forward and reverse. The variation of rotor resistance resulting from temperature change and saturation of inductance is an important issue that must be taken into account, when controlling the induction motor. The ANN can be learned to take these changes into account. That is why, the most important advantage of employing a neural network controller is that, it will be insensitive to system parameter variations, and is able to perform the critical function of slip estimation

internally in a small time and V_{dq} to V_{abc} and i_{abc} to i_{dq} . ANNs can be used in the field-weakening region, where the available power will be constant, without exceeding the voltage rating of the machine. The performance of the ANN was found to match at wide speed and torque ranges, in both directions; forward and reverse. It is then possible to use an ANN controller in a conventional (IFOC) that will be insensitive to system parameter variation and take the advantages of; the learning capability of the ANN, the extremely fast parallel computation, the fault tolerance characteristics due to distributed network intelligence, and achieve the same performance. It can be concluded that, the advantage of using ANNs to perform the function of the IFOC is strictly economic; as in mass production of vector controlled-induction motors; instead of using several DSPs, one for each induction motor, it is possible to use one ANN controller that can cope with identical motors by simply retraining the proposed ANN without changing its structure.

REFERENCES

1. B. K. Bose, "Power Electronics and AC Drives" Prentice-Hall, Upper Saddle River, NJ, 1986.
2. Paresh C. Sen, fellow, IEEE, "Electric Motor Drives and Control-Past, Present, and Future", IEEE Trans. Indus. Electron., Vol. 37, no. 6, Dec.1990.
3. A. M. Trzynadlowski, "The field Orientation Principle in Control of Induction Motors", Kluwer Academic Publishers, Norwell, MA, 1994.
4. F. Blaschke, "The Principle of Field Orientation as Applied to the New Transvektor Closed-Loop Control System for Rotating-Machines", Siemens Review, Vol. 39, no. 5, pp. 217 – 220, 1972.
5. Pekka Tiitinen, Pasi Pohjalainen, and Jarkko Lalu, "The Next Generation Motor Control Method: Direct Torque Control, DTC", ABB Industry On Power Electronics, Research and Development Department, Helsinki, Finland, Oct. 94.
6. A. Hughes, J. Corda, and D. A. Andrade "An Inside Look at Cage Motors with Vector Control", EMD, pp. 258-264, 1993.
7. K. Hasse, "Zur Dynamik Drelrzahleregelter Antriebe mit stromichtergespeisten Asynchon-Kuzschu Laufermaschimes" Darmstadt, Techn.Hochsch., Diss.,1969
8. Y. S. Kung, C. M. Liaw, and M. S. Ouyang, "Adaptive Speed Control for Induction Motor Drives Using Neural Networks", IEEE Trans. Ind. Electronics, Vol. 42, pp. 25-32, Feb. 1995.

9. D. L. Saherzuk, and P. Z. Grabowski, "DSP Implementation of Neural Network Speed Estimator for Inverter fed Induction Motor", in Conf. Rec. IEEE IECON98, pp. 981-985, 1998.
10. M. R. Buhl and R. D. Lorenz, "Design and Implementation of Neural Networks for Digital Current Regulation of Inverter Drives", in Conf. Rec. IEEE-IAS, Annu. Meeting, pp. 415-421, Oct. 1991.
11. L. R. Valdenebro, J. R. Hernandez, and E. Bim, "A Neuro-Fuzzy Based Parameter Identification of an Indirect Vector-Controlled Induction Motor Drive", in Proc. IEEE/ASME Int. Conf. Advanced Intelligent Mechatronics, pp. 347-352, 1999.
12. M. Mohamadian, Ed Nowichi, F. Ashrafzadeh, A. Chu, R. Sachdeva, and Ed Evanik, "A Novel Neural Network Controller and Its Efficient DSP Implementation For Vector-Controlled Induction Motor Drives", IEEE Trans. Ind. App., Vol. 39, no. 6, November/December 2003.

List of symbols

i_{ds}^e, i_{qs}^e	synchronous frame d-q stator currents, A
i_{ds}^s, i_{qs}^s	stationary frame d-q stator currents, A
i_{dr}^e, i_{qr}^e	synchronous frame d-q rotor currents, A
i_{ds}^{e*}, i_{qs}^{e*}	d-q stator reference command currents, A
L_s, L_r	stator and rotor self inductance per phase, H
L_m	mutual inductance, H
R_s, R_r	stator and rotor phase resistance, Ω
T_L, T_e	load torque and developed torque, Nm
V_{as}, V_{bs}, V_{cs}	stator phase voltages, volt
ω_r, ω_r^*	actual and command rotor speed, rad/sec
V_{ds}^e, V_{qs}^e	synchronous frame d-q stator voltages, V
V_{ds}^s, V_{qs}^s	stationary frame d-q stator voltages, V
ω_e, ω_{sl}	synchronous and, slip speed, rad /sec
ψ_{dr}^e, ψ_{qr}^e	synchronous frame d- and q- rotor flux linkages, wb

استخدام الشبكات العصبية الاصطناعية للتحكم في النظام المتجهي لمحركات الحث تستخدم التطبيقات الصناعية المختلفة المحركات المدارة بسرعات متغيرة ولمحرك الحث المغناطيسي العديد من المميزات منها الصلابة واستمرارية الأداء والتكلفة المنخفضة مقارنة بالمحركات الأخرى مما يجعله أكثر ملائمة للاستخدامات التطبيقية إلا أنه يتميز بخصائص تحكم غير خطية متغيرة مع الزمن والتي يصعب معها التحكم في السرعة مما يصعب التحكم في محرك الحث المغناطيسي بالطرق التقليدية حيث أن عزم الإدارة يعتمد على كلاً من الفيض المغناطيسي المتولد وسرعة دوران العضو الدوار. هناك العديد من الطرق الحديثة التي تستخدم للتحكم في محرك الحث المغناطيسي والتي تجعله منافس جيد لمحرك التيار المستمر من حيث سهولة التحكم في سرعته. وأكثر هذه الأنواع استقراراً مع تغير معطيات المحرك من مقاومة ومعاوقة في ظل ظروف التشغيل هو التحكم الغير مباشر في متجه الجهد والمبنى على توجيه مجال العضو الثابت. شملت هذه الأطروحة تطبيق لعلم الشبكات العصبية الاصطناعية على محرك الحث المغناطيسي المتحكم فيه بطريقة التحكم الغير مباشر في متجه الجهد. كما تتضمن كيفية تكوين بناء لثلاث شبكات عصبية تقوم معاً بمحاكاة نظام التحكم المتجهي الغير مباشر كما يبين كيفية تدريبها للتعامل مع البيانات الواردة إليها، وكذلك تم وضع نموذج المقترح في ظرف تشغيل تحاكي الواقع للتحقق من قدرة الشبكات العصبية على تسجيل معدلات استجابة سريعة للسرعة والعزم.